

تخصيص الطيف الترددي لنظام التصميم بتقسيم التردد التعامدي في الشبكات الضوئية

أنور خليفة اليتامي

قسم هندسة الكمبيوتر - جامعة الكويت

الخلاصة

لقد أصبح استخدام تقنية التصميم بتقسيم التردد التعامدي (OFDM) في شبكات الألياف الضوئية هي الطريقة المستقبلية لتلبية احتياجات التطبيقات المتنوعة وذات الترددات المكثفة. حيث يستوعب التصميم بتقسيم التردد التعامدي (OFDM) في شبكات الألياف الضوئية من التطبيقات ذات المتطلبات الصغيرة الى المتطلبات الضخمة. ويعتبر التوجيه وتخصيص الطيف الترددي (RSA) من أهم عوامل نجاح التصميم بتقسيم التردد التعامدي (OFDM) في شبكات الألياف الضوئية. نقدم في هذا البحث طريقتين لتخصيص الطيف الترددي في حالة عدم معرفة وثبات المتطلبات في الشبكة الضوئية. أولاً: تخصيص الطيف الترددي بدءاً من الحواف وثانياً: تقسيم الطيف بناءً على سعة الاحتياجات بحيث يتم في كل مجموعة التنافس للحصول على الحوامل الجزئية في اتجاهين متعاكسين. لقد تم استخدام نتائج المحاكاة لإظهار كفاءة الطرق المقترحة.

Dynamic spectrum allocation in orthogonal frequency-division multiplexing optical networks

ANWAR ALYATAMA

Computer Engineering Department, Kuwait University, P. O. Box 5969, Safat 13060, Kuwait a.yatama@ku.edu.kw

ABSTRACT

Orthogonal frequency-division multiplexing has emerged as a technology that can meet the requirements of diverse, bandwidth-intensive applications envisioned in future optical networks. In orthogonal frequency-division multiplexing optical networks, multiple subcarriers can be allocated to accommodate both subwavelength and superwavelength traffic. An important factor in the success of orthogonal frequency-division multiplexing is routing and spectrum allocation. In this paper, we propose two spectrum allocation algorithms for dynamic orthogonal frequency-division multiplexing optical-based networks: first-fit spectrum allocation starting from the spectrum boundary and spectrum partitioning. In spectrum partitioning, the spectrum is divided into multiple sectors, in which a subset of relative call type sizes compete for the subcarriers in opposite directions. We present simulation results to show the efficiency of our new algorithms.

Keywords: Orthogonal frequency-division multiplexing; routing and spectrum allocation.

INTRODUCTION

Orthogonal frequency-division multiplexing (OFDM) was recently proposed as a modulation technique for optical networks because of its good spectral efficiency and impairment tolerance. Optical OFDM is much more flexible than traditional wavelength-division multiplexing (WDM) systems, enabling elastic bandwidth transmissions (Christodoulopoulos *et al.*, 2010a). An OFDM-based optical network divides a communication channel into a number of equally spaced frequency bands, and a subcarrier carrying a portion of the user information is transmitted in each band. Each of these subcarriers is orthogonal (independent of the others). A major advantage of OFDM over conventional frequency-division multiplexing (FDM) is the exploitation of orthogonality in time, which allows overlapping of signal spectra in the frequency domain (Figure 1).

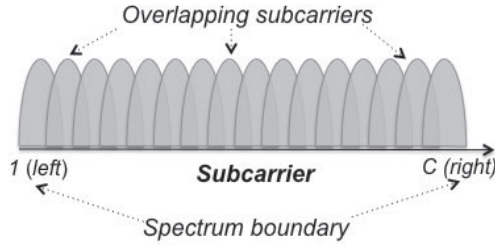


Fig. 1. In an OFDM, data are transmitted on a number of subcarriers in parallel. A major advantage of OFDM over conventional FDM is the exploitation of orthogonality in time, which allows overlapping of signal spectra in the frequency domain. The optical spectrum starts from subcarrier 1 and ends at subcarrier C (*spectrum boundary*).

Future optical networks will need to transport a wide variety of traffic ranging from several tens of gigabits up to terabits per second in a cost-effective and scalable manner (Jinno *et al.*, 2009; Gerstel *et al.*, 2012). OFDM can accommodate both subwavelength and superwavelength traffic by allocating an appropriate number of subcarriers while providing high signal quality and mitigating various impairments (Wang *et al.*, 2011). However, this new concept poses new challenges on the networking level because the routing and wavelength assignment (RWA) algorithms of traditional WDM networks are no longer directly applicable. The wavelength continuity constraint of traditional WDM networks is transformed to a spectrum continuity constraint. Moreover, a connection requiring a capacity larger than one OFDM subcarrier has to be allocated a number of contiguous subcarrier slots (Christodoulopoulos *et al.*, 2010a). Routing and spectrum allocation (RSA) is NP-hard, and it is computationally demanding even for small networks (Klinkowski & Careglio, 2011).

RSA algorithms are used during the planning phase (offline RSA) or the operation phase (dynamic RSA). In the offline RSA problem, planners calculate the spectrum needed to satisfy each demand of a given traffic matrix. Most researchers propose an integer linear programming formulation of RSA that is based on the assignment of channels. For more details about the planning phase, we refer the reader to Ahamed (2008), Zheng *et al.* (2010), Bocoï *et al.* (2009), and Klekamp *et al.* (2010). In this study, we turn our attention to the operational phase (dynamic RSA), in which the demands are not known in advance, and connections (calls) are continuously established and dropped. In dynamic RSA, the spectral route from the source to the destination is determined, when the two end nodes want to communicate. Thus, routing and spectrum allocation are not fixed, and any feasible route and subcarriers from the source node to the destination node are candidates. A dynamic RSA algorithm can be adjusted to changing traffic patterns with time, as traffic at various links or nodes peaks at different hours.

Many heuristic approaches have been proposed for the RWA problem in traditional WDM, some of which can be adopted for the RSA problem in OFDM optical networks (Zang, *et al.*, 1999), with some adjustments needed to comply with the new constraints. For example, instead of a wavelength continuity constraint in WDM, a spectrum continuity constraint arises in OFDM. Moreover, a connection that requires a capacity larger than one OFDM subcarrier has to be assigned a number of contiguous subcarrier slots (Christodoulopoulos *et al.*, 2010a). In this work, we explore only spectrum allocation in dynamic OFDM networks. We assume that the RSA problem is decomposed into two subproblems: the routing (multicommodity) phase and spectrum allocation phase. Routing is assumed to be solved and calculated in the routing phase (Christodoulopoulos *et al.*, 2010a). In this work, we assume that routing follows either a fixed alternate or a load-sharing routing model. In both cases, the set of shortest paths is computed for each source–destination pair by Dijkstra’s algorithm and stored at each source node. The source will first try the direct link connecting the source and the destination. If it is not available, the source node will select a path from the set of the shortest paths in a fixed sequence (fixed alternate) or randomly (load sharing).

The rest of the paper is organized as follows: First, we introduce the network model, traffic assumptions, and performance measurements. In the second section, we review the known spectrum allocation methods for dynamic OFDM. Next, we describe our proposed solution for spectrum allocation and then illustrate some numerical results. We present our conclusions and future research in the last section.

NETWORK MODEL AND PERFORMANCE MEASUREMENTS

The basic unit of real-time network traffic is considered to be one call, and each call originates from a source node s and is directed to a destination node d . The link capacities are uniform with C subcarriers. There are I different call types that have different bandwidth requirements (bit rates), which can be the result of a quantization process, as described in Lea & Alyatama (1995). Because the available optical spectrum, e.g., the C band, is divided into frequency slots of a fixed spectral width, e.g., 25 GHz, 12.5 GHz, or even 6.25 GHz, calls can be allocated to a variable number of these slots as a function of the requested bit rate, applied modulation technique, and slot width (Castro *et al.*, 2012). Hence, each call type i requires T_i contiguous subcarriers. For example, the Telefonica national network has links that can transport a capacity of 4 THz with connection requests having a bit rate uniformly selected from among rates of 40, 100, 160, 400, and 600 Gb/s (Politi *et al.*, 2012). The arrival process of a type i call entering the network and directed to the source–destination pair (s, d) is assumed to be Poissonian with a rate of $\lambda_i(s, d)$ calls/unit time. The holding time of the connection is exponentially distributed with a mean value equal to one unit of time (e.g., 2 h) (Castro *et al.*, 2012). Here, we assume that blocked calls are lost

and do not attempt to re-enter the system, and we also assume that the call connection and disconnection times are short in comparison to the call holding time; hence, these times are neglected. We define the network offered load as (Lea & Alyatama, 1995)

$$\text{Network Offered Load} = K \sum_{i=1}^I \sum_{(s,d)} T_i \lambda_i(s, d), \quad (1)$$

where K is a load factor. A higher load factor K means the network is under heavy traffic, and a small value means the network is under light traffic conditions. The call type distribution function $A(i)$ is defined as the ratio of the type i arrival rate to the total arrival rate of all calls, i.e.,

$$A(i) = \frac{\sum_{(s,d)} \lambda_i(s, d)}{\sum_{i=1}^I \sum_{(s,d)} \lambda_i(s, d)}. \quad (2)$$

The type i call demand function $D(i)$ is defined as the total arrival rate over all source–destination pairs for a type i call multiplied by the number of subcarriers needed to carry the call, i.e.,

$$D(i) = T_i \sum_{(s,d)} \lambda_i(s, d), \quad (3)$$

and the type i normalized call demand function $\bar{D}(i)$ is

$$\bar{D}(i) = \frac{D(i)}{\sum_I D(i)}. \quad (4)$$

The normalized call demand function $\bar{D}(i)$ is used to rationalize the network capacity between different call types. In any network, one important performance measure of the quality of service for real-time services as far as the user is concerned is the end-to-end blocking probability $b_i(s, d)$ (also called the type i node-to-node grade of service, GOS), which is the blocking probability for type i calls originating at a node s and destined for another node d . The targeted network blocking probability (GOS) ranges from 1% to 10% (Dlamini, 2007).

The most common criterion used to measure the network performance is the overall network gain. This is the sum over all source–destination pairs of the probability of accepting a call, multiplied by the worth of such a call for all call types. Assuming the call worth equals the call capacity, then

$$\text{Network gain} = K \sum_{i=1}^I \sum_{(s,d)} \lambda_i(s, d) T_i (1 - b(s, d)), \quad (5)$$

and the normalized network gain is

$$\text{Normalized network gain} = \frac{\text{Network gain}}{\text{Network Offered Load}}. \quad (6)$$

It is worth mentioning that accepting call types requiring less bandwidth usually generates more revenue. Therefore, some load ratios with the same total offered load will generate more revenue than others.

To measure fairness in the network, we use the fairness index (FI) presented in Alyatama (2004),

$$FI = \frac{(\sum_{\forall n} b_i(s, d))^2}{(n \sum_{\forall n} b_i^2(s, d))}, \quad (7)$$

where n is the total number of calls in the network. Our goal is to obtain equal end-to-end blocking probabilities $b_i(s, d)$ for all calls; thus, we attempt to limit the variance to being close to zero, i.e.,

$$\left(\frac{1}{n} \sum_{\forall n} b_i(s, d)\right)^2 - \left(\frac{1}{n} \sum_{\forall n} b_i^2(s, d)\right) \approx 0. \quad (8)$$

The FI is defined as being between 0 and 1, with 1 representing the greatest fairness.

SPECTRUM ALLOCATION ALGORITHMS

In this section, we explore the dynamic spectrum allocation problem; i.e., given a connection that requires T_i subcarriers on a selected route, allocate the starting subcarrier frequency f such that the spectrum continuity constraint is not violated, while maximizing the network gain. In the following spectrum allocation methods, the set of all contiguous subcarriers (in addition to the guard bands) that are available on the selected route is first compiled and indexed. Then, each method will select one set, based on the selection criteria (Diao & Li, 2007; Min *et al.*, 2010). Recall that we assume that the routing is solved, and either a fixed alternate or a load-sharing model is used.

Random spectrum allocation

Among the available sets, one is chosen randomly (usually with uniform probability).

First-fit spectrum allocation

The sets are searched in a fixed order, usually starting from the left (subcarrier 1) or the right (subcarrier C), as shown in Figure 2. Among the available sets, the one with the lowest (highest) index in the fixed order is chosen. The first-fit algorithm is the most effective simple spectrum allocation technique for OFDM-based optical networks because it packs the used spectrum (e.g., at one side) to increase the number of bypassed contiguous subcarriers in a given path (Jinno *et al.*, 2009; Klinkowski & Careglio, 2011). Subsequently, many researchers considered it to solve the dynamic

spectrum allocation problem in OFDM-based optical networks (Castro *et al.*, 2012; Shen & Yang 2011; Christodouloupoulos *et al.*, 2010a; Jinno *et al.*, 2009; Takagi *et al.*, 2011; Wan *et al.*, 2012; Shirazipourazad *et al.*, 2013a; Shirazipourazad *et al.*, 2013b; Yi *et al.*, 2013; Chen *et al.*, 2013).

Least used spectrum allocation

Among the available sets, the one that is the least used in the network is chosen in an attempt to balance the load among all the sets. This scheme also incurs additional storage and computation cost.

Most used spectrum allocation

Among the available sets, the one that is the most used in the network is chosen in an attempt to pack calls into fewer sets. It is the opposite of the least used method; however, the communication overhead, storage, and computation costs are all similar to those of the least used method.

Best-fit spectrum allocation

Among the available sets, the one that is the smallest block of unallocated subcarriers in which a call will fit is chosen. This strategy produces the smallest leftover.

Worst-fit spectrum allocation

Among the available sets, the one that is the largest block of unallocated subcarriers in which a call will fit is chosen. This strategy produces the largest leftover (Silberschatz *et al.*, 2001).

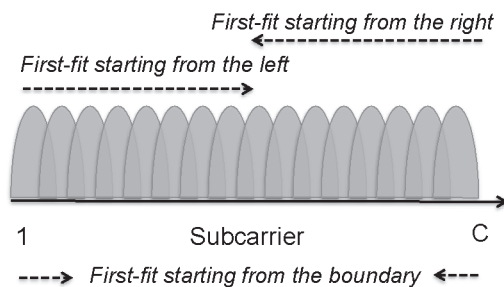


Fig. 2. First-fit spectrum allocation algorithm with different ordering and starting frequencies.

PROPOSED SOLUTION

First, we found that the best order for the first-fit spectrum allocation algorithm begins at the optical spectrum boundary (1, C, 2, C-1, etc.) and proceeds toward the middle (C/2), instead of starting at the left (subcarrier 1) or right (subcarrier C) of the optical spectrum, as shown in Figure 2. To illustrate this, assume that there are L continuous subcarriers in a link. The most likely situation is that, this group will be to the right of the pack if the subcarriers are ordered from the left, to the left of the pack if they are ordered from the right, and in the middle if they are ordered from the spectrum boundary. The group grows in size only when, in the first case, a call directly to the left of this group departs, in the second case, a call directly to the right of this group departs, and in the third case, a call directly to the left or to the right of this group departs. Thus, the chance that a future call of size $> L$ is accepted is more likely in the third case than in the first two cases.

Now, we propose another solution to the spectrum allocation problem in dynamic OFDM. The set of subcarriers is partitioned among different call types into multiple sectors. In each sector, a group of call types will compete for the subcarrier using first-fit starting from the spectrum boundary; i.e., one subgroup will start from the left, and the other subgroup will start from the right. Each sector contains types of relative sizes and/or multiples of a size. The problem of spectrum allocation in OFDM is similar to the problem of packing irregular sizes. Packing calls with less variation is more efficient than packing calls with more diverse sizes, and thus minimizes the bandwidth fragmentation. Fragmentation exists when the total number of subcarriers is sufficient to satisfy a call request, but the available subcarriers are not contiguous (Gokey, 1997; Nutt, 1997). Fragmentation is strongly related to the randomness (entropy) of the call type density function $A(i)$. The uniform distribution has the largest entropy and can be considered the worst case.

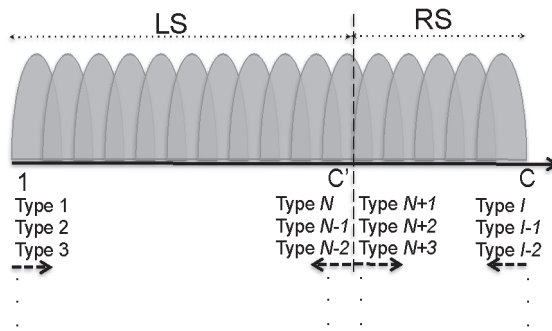


Fig. 3. Proposed spectrum allocation algorithm partitions a spectrum with C subcarriers into two sectors. The left sector starts at subcarrier 1 and ends at subcarrier C' , whereas the right sector starts at subcarrier $C' + 1$ and ends at subcarrier C . In each sector, calls compete for the subcarriers in opposite order.

The size of each sector is relative to the sum of the normalized call demand function $\bar{D}(i)$ belonging to the sector.

In this work, we propose to partition a spectrum with C subcarriers into two sectors, the left sector (LS) with C' subcarriers and the right sector (RS) with $C - C'$ subcarriers (Figure 3). The LS has $N = \lfloor \frac{I}{2} \rfloor$ call types with the largest sizes, and the RS has $I - N$ call types with the smallest sizes. The LS starts at subcarrier 1 and ends at subcarrier C' , whereas the RS starts at subcarrier $C' + 1$ and ends at subcarrier C . In each sector, calls are competing for the subcarriers in the opposite order; i.e., half of them will start the sequence from left to right, and the other half will start the sequence from right to left. The size of the sectors represents a tradeoff between reducing the call type size differences and maximizing the resource sharing. Further, sectors are not of equal size, and a simple way to calculate the size of each sector is to partition the available spectrum according to the demand for each type, $\bar{D}(i)$, given in Equation (4). The assigned subcarriers in each sector are rounded up or down to the nearest multiple of the call sizes ($\sum T_i$) in the sector. Hence, $C' \approx \sum_{i \leq \lfloor \frac{I}{2} \rfloor} \bar{D}(i) \times C$. The pseudo-code is shown in Algorithm 1, and examples are shown in the next section.

Finally, the work in (Christodoulopoulos *et al.*, 2010b) showed that an appropriate ordering for the subcarriers is crucial to produce near-optimal performance for the offline (planning) problem of an OFDM-based optical network. They introduced the most subcarrier first ordering, where the connection demands are first ordered in decreasing order of the number of their requested subcarriers, and the demand that requires the most subcarriers is served first. Thus, calls requesting a high number of subcarriers are packed at one side of the optical spectrum, and those requesting fewer subcarriers are packed at the other side, creating separate virtual sectors based on the call size T_i .

Algorithm 1 The main steps used to divide the frequency spectrum into two sectors and define the spectrum allocation sequence for each call type.

Input: $C, I, T, \lambda \forall s, d, i=1, \dots, l$.

Output: C' and the spectrum allocation sequence for each call type $i=1, \dots, l$

1. Calculate $\Lambda(i) \forall i=1, \dots, l$ using Equation 2.
2. Calculate $D(i), \overline{D}(i)$ using Equations 3, 4.
3. Dedicate $\lfloor \frac{I}{2} \rfloor$ call types with the largest size to the left sector (LS) and $\lfloor \frac{I}{2} \rfloor$ call types with the smallest size to the right sector (RS).
4. Assign D' subcarriers to the left sector (LS) and $C-C'$ subcarriers to the right sector (RS) where $C' \approx \sum_{i \leq \lfloor \frac{I}{2} \rfloor} \overline{D}(i) \times C$ (after rounding up or down to the nearest multiple of the call sizes in the sector).
5. **for** $i=1$ to $\lfloor \frac{I}{4} \rfloor$
 The spectrum allocation for call type i will search for the available spectrum starting at subcarrier 1 and proceeding toward C' (*left to right*).
6. **endfor**
7. **for** $i = \lfloor \frac{I}{4} \rfloor$ to $\lfloor \frac{I}{2} \rfloor$
 The spectrum allocation for call type i will search for the available spectrum starting at subcarrier C' and proceeding toward 1 (*right to left*).
8. *endifor*
9. *for* $i = \lfloor \frac{I}{2} \rfloor$ to $\lfloor \frac{3I}{4} \rfloor$
 The spectrum allocation for call type i will search for the available spectrum starting at subcarrier $C'+1$ and proceeding toward C (*left to right*).
10. **endfor**
11. **for** $i = \lfloor \frac{3I}{4} \rfloor$ to I
 The spectrum allocation for call type i will search for the available spectrum starting at subcarrier C and proceeding toward $C'+I$ (*right to left*).
12. **endfor**

NUMERICAL RESULTS

To test our proposed spectrum allocation algorithms, we present the 14-node NSFNET network topology shown in Figure 4. The routing algorithm assumes a fixed order of direct and alternate routes between the source and the destination. We assume a subcarrier capacity of 10 Gbps, which represents one frequency unit. The

link capacities are uniform with $C = 400$ subcarriers, i.e., 4 Tbps. The network has equal source–destination traffic flows, and the call bit rates are 1 Tbps, 400 Gbps, 100 Gbps, 40 Gbps, or 10 Gbps, which demand T_i subcarriers of 100, 40, 10, 4, or 1 frequency units, respectively. Different traffic type distributions $A(i)$ are considered: uniform, negative exponential, and bell-shaped (Figure 5). These three distributions were chosen not because they resemble any traffic type distribution in OFDM, but for their representativeness in stochastic analysis, including the worst-case scenario. In the uniform distribution, the arrival rate of a type i call is uniform, i.e., $A(i) = 0.2$, whereas for the negative exponential distribution, the arrival rate of type i calls is a negative exponential of the size of the type i call, i.e., $A(i) = e^{-0.05 T_i}$. For the bell-shaped distribution, 40% of the arrival rate is for calls requiring 10 subcarriers, 20% of the arrival rate is for calls requiring either 40 or 4 subcarriers, and 10% of the arrival rate is for calls requiring either 1 or 100 subcarriers.

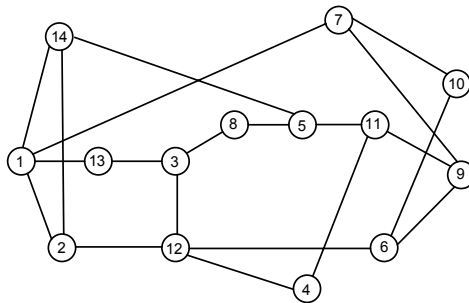


Fig. 4. Fourteen-node NSFNET network topology.

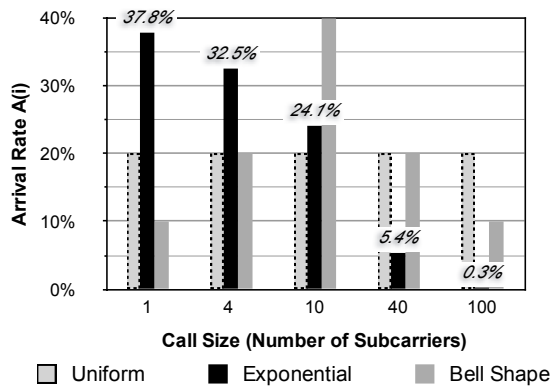


Fig. 5. Different traffic type distributions $A(i)$ are considered: uniform, negative exponential, and bell-shaped.

Simulations are performed and repeated 10 times, with each run starting with a different random seed. The averaged result is obtained with 95% confidence with a confidence interval within 1% of the average value.

For our proposed spectrum allocation algorithm, we partition the link capacity into two sectors. The RS has the smallest call types, i.e., $T_i = \{1, 4, 10\}$, and the LS has the largest sizes i.e., $T_i = \{40, 100\}$. Call types with sizes of 1, 4, and 10 start from the right side of the sector, whereas call types with sizes of 10 and 100 start from the left side. Table 1 shows a simple calculation for partitioning the spectrum into the two sectors based on the call demand for the uniform call type distribution $A(i) = 0.2$. The assigned subcarriers are rounded up or down to the nearest multiple of the call sizes in the sectors. The sector sizes are not related to the network load factor. Figure 6 shows the spectrum subcarrier sequence for each call type with the uniform call type distribution. Tables 2 and 3 show the same simple calculation for the exponential and bell-shaped call type distributions $A(i)$.

Table 1. Spectrum partitioning for uniform call type distribution.

Sector	T_i	A(i)	D(i)	$\bar{D}(i)$	$\bar{D}(i) \times C$	Assigned Subcarriers
Right	1	20%	0.2	0.6%	3	40
	4	20%	0.8	2.6%	10	
	10	20%	2	6.5%	26	
Left	40	20%	8	26%	103	360
	100	20%	20	65%	258	

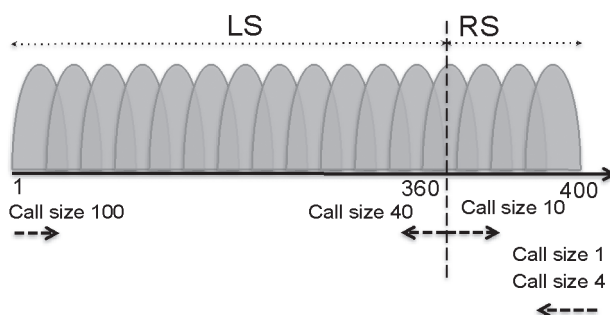


Fig. 6. Spectrum subcarrier sequence for each call type for the uniform type traffic distribution.

Table 2. Spectrum partitioning for exponential call type distribution.

Sector	T_i	A(i)	D(i)	$\bar{D}(i)$	$\bar{D}(i) \times C$	Assigned Subcarriers
Right	1	37.8%	0.38	6%	3	230
	4	32.5%	1.3	20%	10	
	10	24.1%	2.41	37%	26	
Left	40	5.4%	2.16	33%	103	140
	100	0.3%	0.27	4%	258	

Table 3. Spectrum partitioning for bell-shaped call type distribution.

Sector	T_i	A(i)	D(i)	$\bar{D}(i)$	$\bar{D}(i) \times C$	Assigned
Right	1	10%	0.1	0.4%	2	80
	4	20%	0.8	3%	14	
	10	40%	4	17%	70	
Left	40	20%	8	35%	140	320
	100	10%	10	44%	175	

In Figure 7, we plot the normalized network gain against different load factors for the uniform call type distribution $A(i) = 0.2$. Different load factors K are considered to cover the targeted GOS between less than 1% (light load) to more than 10% (overload).

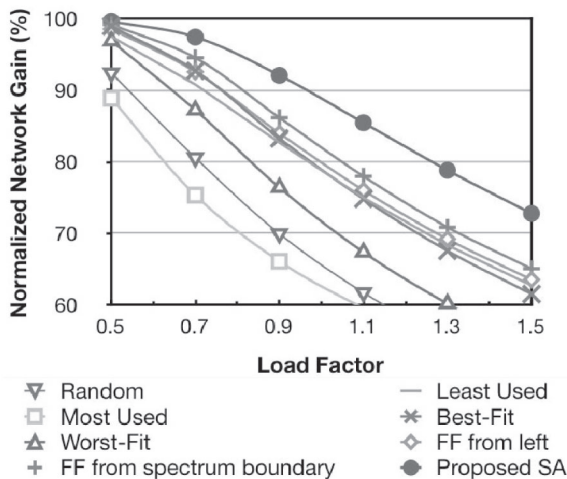


Fig. 7. Normalized network gain for 14-node NSF network with uniform call type distribution for different network load factors K.

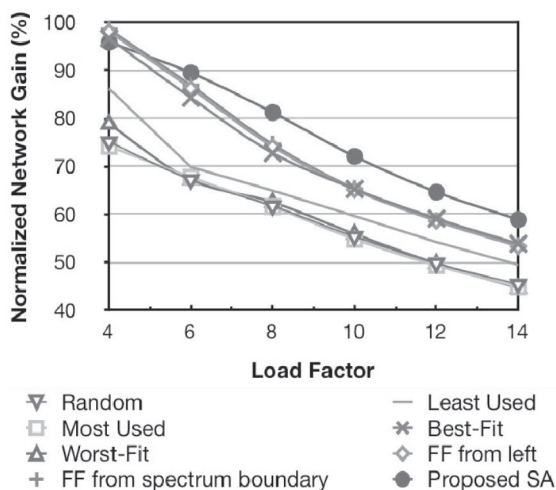


Fig. 8. Normalized network gain for 14-node NSF network with exponential call type distribution for different network load factors K .

Figures 8 and 9 show the same performance parameters for the exponential and bell-shaped call type distributions. The figures show that our proposed spectrum allocation is superior to the other algorithms. The worst spectrum allocation algorithms are most used, random, and worst-fit. The figures also show that first-fit starting from the spectrum boundary is better than first-fit starting from the left. The results for first-fit starting from the left and starting from the right are similar because our link capacities are uniform. Moreover, algorithms that pack the call requests (e.g., first-fit) tend to outperform those that spread the call requests (e.g., random). Finally, minimizing the average overall blocking probability is not the same as maximizing the overall network gain in this multirate environment. Thus, the average overall blocking probability for our proposed spectrum allocation algorithm may be higher because of the equal call demand sector calculation approach.

Figures 10, 11, and 12 show the FI for the three different call type distributions. In general, the FI for our proposed algorithm is higher because we minimized the competition between calls with a small capacity request and those with larger requests for the same resources. Furthermore, the blocking probabilities of all the call types are almost the same because of the way we partitioned the spectrum on the basis of equal call demands. Our algorithm is shown here to have the best performance with the best fairness. An exception is the light to moderate load for the exponential traffic type distribution, in which the top three SA algorithms in terms of network gain had lower FI. In this case, most of the traffic is of size 1 and 4 (70%) with the majority of their end-to-end blocking probabilities almost zero. It is worth mentioning that the FI will not reach one because of the unfairness between calls using a direct link and calls using multiple links.

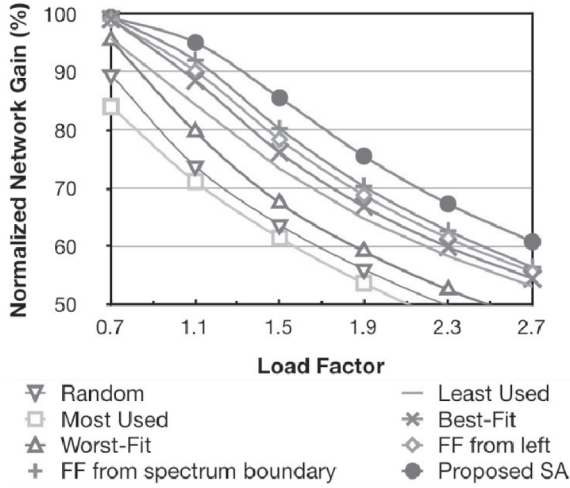


Fig. 9. Normalized network gain for 14-node NSF network with bell-shaped call type distribution for different network load factors K .

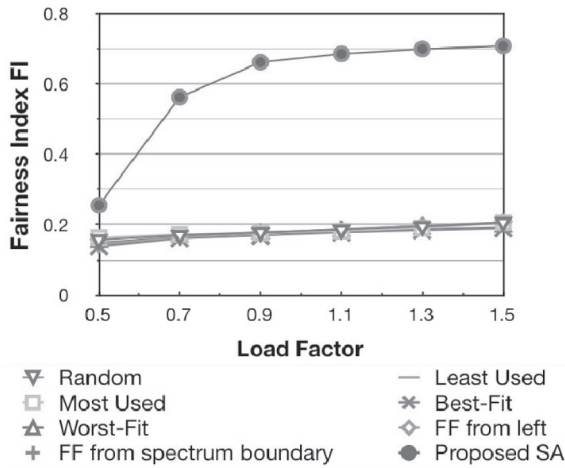


Fig. 10. Fairness index for 14-node NSF network with uniform call type distribution for different network load factors K .

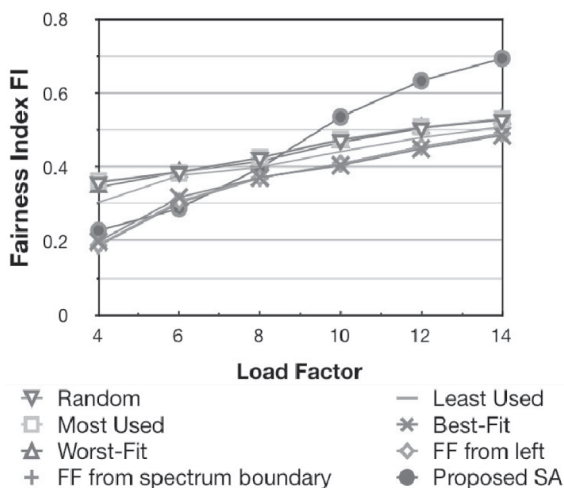


Fig. 11. Fairness index for 14-node NSF network with exponential call type distribution for different network load factors K .

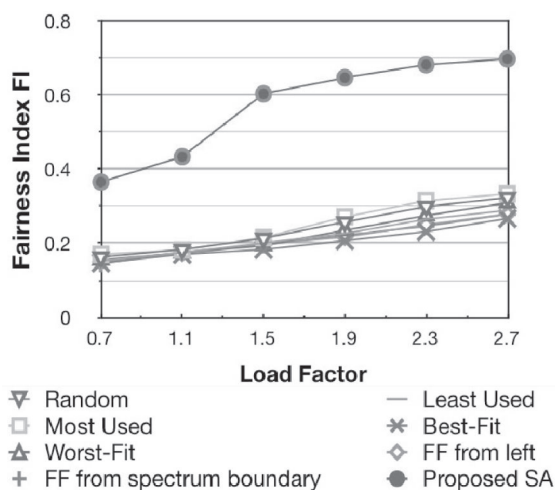


Fig. 12. Fairness index for 14-node NSF network with bell-shaped call type distribution for different network load factors K .

Figures 13 and 14 show the results, when we increase the number of call types from 5 to 10, i.e., $I = 10$. Two cases are considered, with $T_i = \{1, 2, 4, 5, 8, 10, 20, 40, 50, 100\}$ in the first case and $T_i = \{1, 4, 5, 10, 20, 40, 50, 70, 90, 100\}$ in the second. The RS has the smallest call types, and the LS has the largest call types. In both figures, the proposed spectrum allocation algorithm is foremost, and first-fit starting from the spectrum boundary is better than first-fit starting from the left.

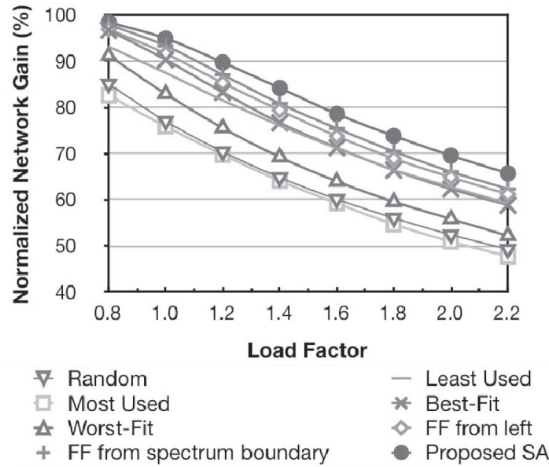


Fig. 13. Normalized network gain for 14-node NSF network with $\beta = 10$ and $T_i = \{1, 2, 4, 5, 8, 10, 20, 40, 50, 100\}$. The call type distribution $A(i)$ is uniform.

To further test our proposed spectrum allocation algorithm, we present the 24-node network shown in Figure 15 with a new routing and traffic distribution. The routing algorithm shares uniformly the offered load between the set of shortest paths computed by Dijkstra’s algorithm. The network source–destination loads are no longer equal and are drawn according to a uniform distribution between 0 and 1. The link capacities are uniform with $C = 400$ frequency units, i.e., 4 Tbps. The spectrum subcarrier sequence for each call type is shown in Figure 6. In Figure 16, we show that the normalized network gain for our proposed spectrum allocation algorithm is superior to that for the other algorithms.

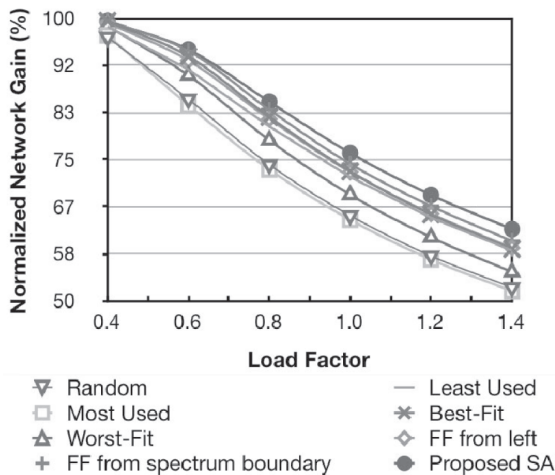


Fig. 14. Normalized network gain for 14-node NSF network with $\beta = 10$ and $T_i = \{1, 4, 5, 10, 20, 40, 50, 70, 90, 100\}$. The call type distribution $A(i)$ is uniform.

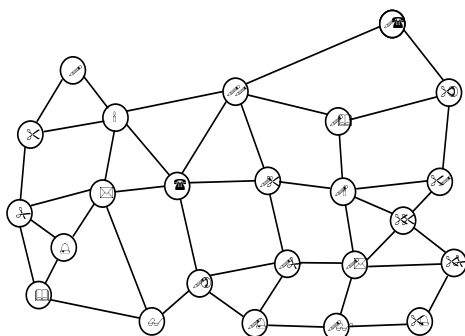


Fig. 15. Twenty-four-node network topology.

Finally, Figure 17 shows the average overall subcarrier utilization, which is defined as the total busy time for each subcarrier, relative to the total time averaged over all network links. The subcarrier utilization decreases as the index increases for first-fit spectrum allocation starting from the left, whereas, it is high on the spectrum boundary for first-fit spectrum allocation starting from the spectrum boundary. For our proposed spectrum allocation method, a step behavior appears, in which a bulk of contiguous subcarriers have the same utilization. For example, in the LS, where we have two calls of size 100 and 40, the step intervals are 100 subcarriers in size on the left and 40 subcarriers in size on the right side of the LS, which follows our sequencing given in Figure 6. Hence, the left-most subcarriers in LS are reserved predominantly for calls with size 100, and the right-most subcarriers in LS are reserved predominantly for calls with size 40. Because calls compete for the subcarriers in the opposite order in each sector, the subcarrier utilization is high on the spectrum boundary and low in the middle of each sector. Finally, the figure also shows that our proposed algorithm obtains the best overall resource utilization.

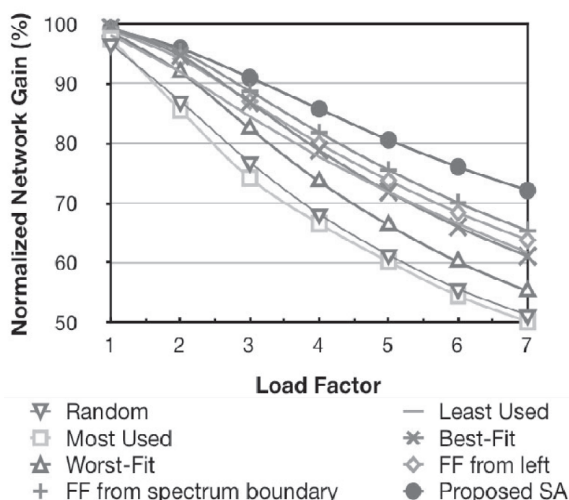


Fig. 16. Normalized network gain for 24-node network for different network load factors K .

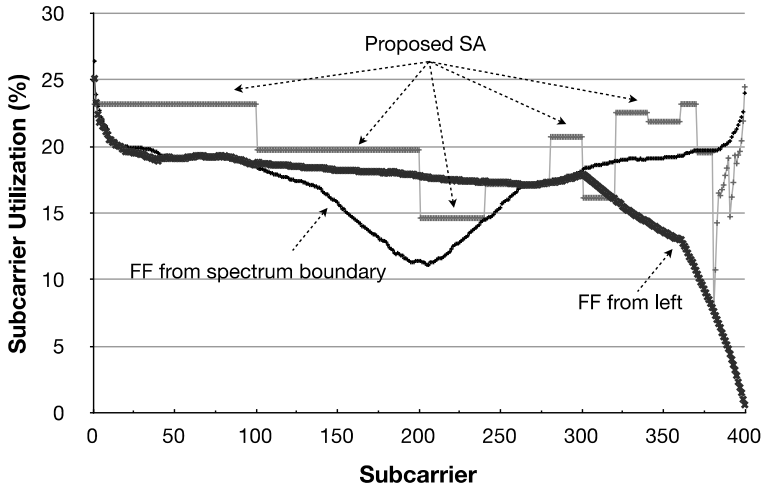


Fig. 17. Average overall subcarrier utilization in 24-node network.

CONCLUSIONS AND FUTURE RESEARCH

We considered the problem of spectrum allocation and presented two algorithms to solve it for a dynamic OFDM network. We initially presented first-fit starting from the spectrum boundary and then proposed a new spectrum allocation algorithm that partitions the bandwidth spectrum into several sectors. In each sector, calls with relative sizes compete for the available subcarriers in opposite order. Simulation results showed that our proposed algorithms outperformed all the other spectrum allocation techniques for a dynamic OFDM network in terms of overall network gain and fairness. In future research, we plan to investigate more techniques and a complicated model to improve the spectrum partitioning. One idea is to place calls in more than one spectrum partition using a load-sharing model or have dynamic boundaries for the spectrum partitioning. However, the simple calculation provided in this work proved the concept of spectrum partitioning.

REFERENCES

- Ahamed, S. 2008. Performance analysis of OFDM, *Journal of Theoretical and Applied Information Technology*, 4(1): 22–30.
- Alyatama, A. 2004. Fairness in WDM optical networks without wavelength conversions, *International Journal on Wireless and Optical Communications*, 2(1): 115–133.
- Bocoi, A., Schuster, M., Rambach, F., Kiese, M., Bunge, C. & Spinnler, B. 2009. Reach-dependent capacity in optical networks enabled by OFDM, *Optical Fiber Communication Conference*, San Diego, CA, paper OMQ4.
- Castro, A., Velasco, L., Ruiz, M., Klinkowski, M., Fernández-Palacios, J. & Careglio, D. 2012. Dynamic routing and spectrum (re)allocation in future elastic optical networks, *Computer Networks*, 56(2): 2869–2883.

- Chen, X., Zhong, Y. & Jukan, A. 2013.** Multipath routing in elastic optical networks with distance-adaptive modulation formats, IEEE International Conference on Communications (ICC).
- Christodouloupoulos, K., Tomkos, I. & Varvarigos, E. 2010a.** Spectrally/bitrate flexible optical network planning, European Conference and Exhibition on Optical Communication, Torino, Italy.
- Christodouloupoulos, K., Tomkos, I. & Varvarigos, E. 2010b.** Routing and spectrum allocation in OFDM-based optical networks with elastic bandwidth allocation, Global Telecommunications Conference (GLOBECOM 2010), **31(1)**: 15-22.
- Diao, Z. & Li, V. 2007.** Fading-Aware packet scheduling algorithm in OFDM-MIMO systems, EURASIP Journal on Wireless Communications and Networking, ID 95917.
- Dlamini, N. 2007.** Teletraffic engineering/Blocking, http://en.wikiversity.org/wiki/Teletraffic_engineering.
- Gerstel, O., Jinno, M., Lord, A. & Yoo, S. 2012.** Elastic optical networking: a new dawn for the optical layer?, IEEE Communications Magazine, **50(2)**: s12–s20.
- Gokey, C. 1997.** Fragmentation Example, <http://asia.cs.bowiestate.edu/cgokey/fragment/example.html>.
- Jinno, M., Takara, H. & Kozicki, B. 2009.** Dynamic optical mesh networks: drivers, challenges and solutions for the future, European Conference and Exhibition on Optical Communication, Vienna, Austria.
- Klekamp, A., Rival, O., Morea, A., Dischler, R. & Buchali, F. 2010.** Transparent WDM network with bitrate tunable optical OFDM transponders, National Fiber Optic Engineers Conference, San Diego, CA, paper NTuB5.
- Klinkowski, M. & Careglio, D. 2011.** A routing and spectrum assignment problem in optical OFDM networks, First European Teletraffic Seminar (ETS), Poznań, Poland, 2011.
- Lea, J. & Alyatama, A., 1995.** Bandwidth quantization and states reduction in the broadband ISDN, IEEE/ACM Transactions on Networking, **3(3)**: 352–360.
- Min, H., Cho, Y. & Hong, J. 2010.** Dynamic memory allocator for sensor operating system design and analysis, Journal of Information Science and Engineering, **26(1)**: 1–14.
- Nutt, G. 1997.** Operating Systems: A Modern Perspective, First Edition, Addison-Wesley, Reading, MA.
- Politi, C., Anagnostopoulos, V., Matrakidis, C., Stavdas, A., Lord, A., López, V. & Fernández-Palacios, J. 2012.** Dynamic operation of Flexi-Grid OFDM-based networks, Optical Fiber Communication Conference, Los Angeles, CA, paper OTh3B.2.
- Shen, G. & Yang, Q. 2011.** From coarse grid to mini-grid to gridless: How much can gridless help contentionless? OFC/NFOEC, Los Angeles, CA.
- Shirazipourzad, S., Chenyang Z., Derakhshandeh, Z. & Sen, A. 2013a.** On routing and spectrum allocation in spectrum-sliced optical networks, INFOCOM 2013.
- Shirazipourzad, S., Derakhshandeh, Z. & Sen, A. 2013b.** Analysis of on-line routing and spectrum allocation in spectrum-sliced optical networks, IEEE International Conference on Communications (ICC).
- Silberschatz, A., Galvin, P. & Gagne, G., 2001.** Operating system concepts, Sixth Edition, John Wiley & Sons, Inc., New York, NY.
- Takagi, T., Hasegawa, H., Sato, K., Sone, Y., Kozicki, B., Hirano, A. & Jinno, M. 2011.** Dynamic routing and frequency slot assignment for elastic optical path networks that adopt distance adaptive modulation, OFC/NFOEC, Los Angeles, CA.
- Wan, X., Hua, N. & Zheng, X. 2012.** Dynamic routing and spectrum assignment in spectrum-flexible transparent optical networks, IEEE/OSA Journal of Optical Communications and Networking, **4(8)**: 603–613.
- Wang, Y., Cao, X. & Pan, Y. 2011.** A study of the routing and spectrum allocation in spectrum-sliced elastic optical path networks, IEEE INFOCOM, Shanghai, China.

- Yi, F., Guo, B., Xin, C., He, Y. & Li, Z. 2013.** Enhanced minimum interference routing algorithms for elastic optical networks, OptoElectron. Communication Conference held jointly with Int. Conf. Photonics in Switch. (OECC/PS).
- Zang, H., Jue, J. & Mukherjee, B. 1999.** A review of routing and wavelength assignment approaches for wavelength-routed optical WDM networks, Optical Networks Magazine, 1: 47–60.
- Zheng, W., Jin, Y., Sun, W., Guo, W. & Hu, W. 2010.** On the spectrum-efficiency of bandwidth-variable optical OFDM transport networks, Optical Fiber Communication Conference, San Diego, CA.

Open Access: This article is distributed under the terms of the Creative Commons Attribution License (CC-BY 4.0) which permits any use, distribution, and reproduction in any medium, provided the original author(s) and the source are credited.

Submitted: 19/12/2013

Revised: 19/03/2014

Accepted: 03/04/2014

مجلة دراسات الخليج والجزيرة العربية



مجلة علمية فصلية محكمة تصدر عن مجلس النشر العلمي - جامعة الكويت
صدر العدد الأول منها في يناير عام 1975م

رئيس التحرير

أ. د. بدر عمر العمر

ترحب المجلة بنشر البحوث والدراسات العلمية المتعلقة بشؤون
منطقة الخليج والجزيرة العربية في مختلف علوم البحث والدراسة .

ومن أبوابها

- البحوث العربية.
- البحوث الإنجليزية.
- ملخصات الرسائل الجامعية:
- ماجستير - دكتوراه.
- عرض الكتب ومراجعتها.
- التقارير : مؤتمرات - ندوات
- البيبلوجرافيا العربية.

الاشتراكات

ترسل قيمة الاشتراك مقدماً بشيك لأمر - جامعة الكويت
مسحوب على أحد المصارف الكويتية

داخل دولة الكويت : للأفراد : 3 دنانير - للمؤسسات : 15 ديناراً
الدول العربية : للأفراد : 4 دنانير - للمؤسسات : 15 ديناراً
الدول الغير عربية : للأفراد : 4 دنانير - للمؤسسات : 15 ديناراً

توجه جميع المراسلات باسم رئيس تحرير مجلة دراسات الخليج والجزيرة العربية

Tel.: (+965) 24833215 - 24984066 - 24984067
www.pubcouncil.kuniv.edu.kw/jgaps

Fax: (+965) 24833705

P.O. Box 17073 Al-Khaldiah, 72451 Kuwait
E - mail : jgaps@ku.edu.kw

www.ku.edu.kw